



Measurement of the $Z+b$ -jet cross-section in pp collisions at $\sqrt{s} = 7$ TeV in the forward region

The LHCb collaboration[†]

Abstract

The associated production of a Z boson or an off-shell photon γ^* with a bottom quark in the forward region is studied using proton-proton collisions at a centre-of-mass energy of 7 TeV. The Z bosons are reconstructed in the $Z/\gamma^* \rightarrow \mu^+\mu^-$ final state from muons with a transverse momentum larger than 20 GeV, while two transverse momentum thresholds are considered for jets (10 GeV and 20 GeV). Both muons and jets are reconstructed in the pseudorapidity range $2.0 < \eta < 4.5$. The results are based on data corresponding to 1.0 fb^{-1} recorded in 2011 with the LHCb detector. The measurement of the Z+b-jet cross-section is normalized to the Z+jet cross-section. The measured cross-sections are

$$\sigma(Z/\gamma^*(\mu^+\mu^-)+b\text{-jet}) = 295 \pm 60 \text{ (stat)} \pm 51 \text{ (syst)} \pm 10 \text{ (lumi) fb}$$

for $p_T(\text{jet}) > 10$ GeV, and

$$\sigma(Z/\gamma^*(\mu^+\mu^-)+b\text{-jet}) = 128 \pm 36 \text{ (stat)} \pm 22 \text{ (syst)} \pm 5 \text{ (lumi) fb}$$

for $p_T(\text{jet}) > 20$ GeV.

Published in JHEP 01 (2015) 064

© CERN on behalf of the LHCb collaboration, license CC-BY-4.0.

[†]Authors are listed at the end of this paper.

1 Introduction

The cross-section for the forward production of a Z boson¹ in association with a bottom quark (referred to as Z+b-jet) is sensitive to the parton distribution functions (PDF) in the proton in a phase-space region poorly constrained by existing measurements. It is a benchmark measurement for perturbative quantum chromodynamics phenomenology of heavy quarks and allows constraints to be placed on backgrounds in studies of the Standard Model (SM) Higgs boson and searches for non-SM physics.

The ATLAS and CMS collaborations reported measurements of Z+b-jet production with jet transverse momentum² larger than 25 GeV and jet pseudorapidity $|\eta| < 2.1$, where they find good agreement with next-to-leading order (NLO) predictions [1, 2]. Similar measurements were performed by the CDF [3] and D0 [4] collaborations at the Tevatron, where the dominant contribution comes from the quark-antiquark interaction. The forward acceptance of the LHCb experiment, with a pseudorapidity coverage in the range $2 < \eta < 5$, probes a kinematic region complementary to that probed by ATLAS and CMS. The LHCb measurements are sensitive to the parton distribution functions in the proton at low and high values of the Bjorken x variable, where the uncertainties are largest.

In this paper we describe the measurement of the production of Z+b-jet with $Z/\gamma^* \rightarrow \mu^+\mu^-$ in proton-proton collisions at $\sqrt{s} = 7$ TeV using the data collected by the LHCb experiment in 2011. The data set corresponds to an integrated luminosity of 1.0 fb^{-1} .

The presence of a bottom hadron candidate is used to tag the jet as originating from a bottom quark, following Ref. [5]. The results are compared to NLO and leading-order (LO) calculations using massless and massive bottom quarks.

2 Detector and samples

The LHCb detector [6] is a single-arm forward spectrometer covering the pseudorapidity range $2 < \eta < 5$, designed for the study of particles containing b or c quarks. The detector includes a high-precision tracking system consisting of a silicon-strip vertex detector surrounding the pp interaction region [7], a large-area silicon-strip detector located upstream of a dipole magnet with a bending power of about 4 Tm, and three stations of silicon-strip detectors and straw drift tubes [8] placed downstream of the magnet. The tracking system provides a measurement of momentum, p , with a relative uncertainty that varies from 0.4% at low momentum to 0.6% at 100 GeV. The minimum distance of a track to a primary vertex, the impact parameter, is measured with a resolution of $(15 + 29/p_T) \mu\text{m}$, where p_T is the transverse momentum in GeV. Different types of charged hadrons are distinguished using information from two ring-imaging Cherenkov detectors [9]. Photon, electron and hadron candidates are identified by a calorimeter system consisting of scintillating-pad (SPD) and preshower detectors, an electromagnetic calorimeter and a hadronic calorimeter. The calorimeters have an energy resolution of

¹Throughout this paper Z boson includes both the Z^0 and the off-shell photon, γ^* , contributions.

²In this paper we use natural units ($c = \hbar = 1$).

$\sigma(E)/E = 10\%/\sqrt{E} \oplus 1\%$ and $\sigma(E)/E = 69\%/\sqrt{E} \oplus 9\%$ (with E in GeV), respectively. Muons are identified by a system composed of alternating layers of iron and multiwire proportional chambers [10]. The trigger consists of a hardware stage, based on information from the calorimeter and muon systems, followed by a software stage, which applies a full event reconstruction [11].

The events used in this analysis are selected by a trigger that requires the presence of at least one muon candidate with $p_T > 10$ GeV. In addition, the hardware trigger requires a hit multiplicity in the SPD less than 600, in order to reject events whose processing in the software trigger would be too time consuming. This retains about 90% of the events that contain a Z boson.

Simulated samples of pp collisions are generated with PYTHIA v6.4 [12] with a specific LHCb configuration [13] using the CTEQ6ll [14] parameterization of the PDFs. Decays of hadronic particles are described by EVTGEN [15], while the interaction of the generated particles with the detector, and its response, are implemented using GEANT4 [16] as described in Ref. [17].

3 Measurement strategy and event selection

The $Z \rightarrow \mu^+ \mu^-$ selection follows that described in Ref. [18]. Muon tracks in the fiducial volume ($2.0 < \eta(\mu) < 4.5$) are required to have transverse momentum greater than 20 GeV. In order to have good quality muons, the relative uncertainty on the momentum of each muon is required to be less than 10% and the χ^2 probability for the associated track fit larger than 0.1%. The dimuon candidate mass is required to be in the 60 – 120 GeV range. The contribution from combinatorial background of $(0.31 \pm 0.06)\%$, evaluated in Ref. [18], is neglected.

Charged and neutral particles are clustered by the anti- k_T algorithm [19] with distance parameter $R = 0.5$ as implemented in the FASTJET software package [20]. As in Ref. [18], the jet energy is corrected to the particle level excluding neutrinos and the same jet quality requirements are applied. The jets are required to be reconstructed within the pseudorapidity range $2.0 < \eta(\text{jet}) < 4.5$ and two transverse momentum thresholds of 10 and 20 GeV are studied. In addition to those kinematic criteria, jets are required to be isolated from the muons of the Z boson decay ($\Delta R(\text{jet}, \mu) > 0.4$), where ΔR is the distance in $\eta - \phi$ space and ϕ is the azimuthal angle.

The Z+b-jet cross-section is determined from the ratio of Z+b-jet to Z+jet event yields corrected for efficiencies and normalized by the Z+jet production cross-section

$$\sigma(\text{Z+b-jet}) = \frac{\varepsilon(\text{Z+jet})}{\varepsilon(\text{Z+b-jet})} \frac{1}{\varepsilon(\text{b-tag})} \frac{N(\text{Z+b-jet})}{N(\text{Z+jet})} \sigma(\text{Z+jet}), \quad (1)$$

where $N(\text{Z+b-jet})$ is the observed number of Z+b-jet events, $N(\text{Z+jet})$ is the number of observed Z+jet events, $\varepsilon(\text{Z+jet})/\varepsilon(\text{Z+b-jet})$ is the ratio of efficiencies for the reconstruction and selection of Z+jet and Z+b-jet events and $\varepsilon(\text{b-tag})$ is the efficiency of the b-tagging. The production cross-section of a Z boson associated with jets, $\sigma(\text{Z+jet})$, was previously

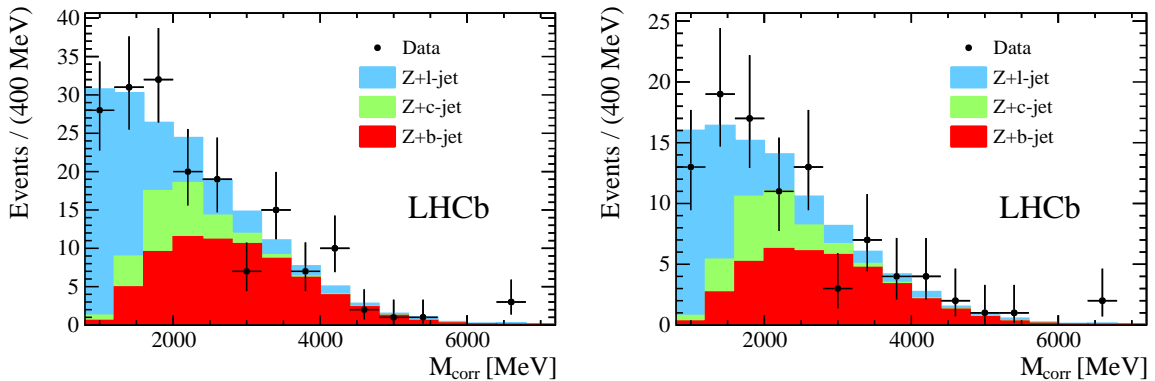


Figure 1: M_{corr} distribution for (left) $p_{\text{T}}(\text{jet}) > 10 \text{ GeV}$ and (right) $p_{\text{T}}(\text{jet}) > 20 \text{ GeV}$. Data (black points) are compared to the template fit results. The uncertainties shown are statistical only.

measured by LHCb [18]. The same data sample, Z boson selection and jet selection are used but identification of jets originating from bottom quarks is added. By using this approach, the systematic uncertainties and the efficiencies are largely the same as those of Ref. [18], except for those related to the b-jet identification.

An algorithm similar to that described in Refs. [5, 21] is used for the identification of secondary vertices consistent with the decay of a beauty hadron, using tracks that form the jet. Topological secondary vertices (TOPO), significantly separated from the primary vertex, are formed by considering all combinations of two, three and four particles within a jet, where particles include both charged particles reconstructed from tracks and reconstructed K_s^0 and Λ hadrons. The requirement of a TOPO candidate greatly reduces the background of jets originating from light partons (l-jets) and charm quarks (c-jets). The number of b-jets is extracted from an unbinned likelihood fit to the corrected mass of the TOPO candidate defined as $M_{\text{corr}} \equiv \sqrt{M^2 + p^2 \sin^2 \theta} + p \sin \theta$. Here, M and p are the invariant mass and momentum of the TOPO candidate and θ is the angle between its momentum direction and the flight direction inferred from the positions of the primary and secondary vertices [11].

Templates for the M_{corr} distribution of b-jets, c-jets and l-jets are obtained from simulation of Z+jet, inclusive b-hadron and inclusive c-hadron production. The shapes of the templates for b-jets, c-jets and l-jets in these samples show no dependence on the production process nor on the p_{T} of the jet. The *sPlot* method [22] is used to estimate the b-jet p_{T} and η spectra. Figure 1 shows the M_{corr} distribution of b-jet candidates with the fit results overlaid.

Jet reconstruction inefficiencies mainly arise from low-momentum particles and calorimeter response, therefore no large differences between jets originating from heavy quarks and from light quarks and gluons are expected. Hence, the ratio $\varepsilon(\text{Z+jet})/\varepsilon(\text{Z+b-jet})$ is assumed to be unity, which is confirmed by simulation.

The b-tagging efficiency, $\varepsilon(\text{b-tag})$, is determined in simulation as a function of the jet

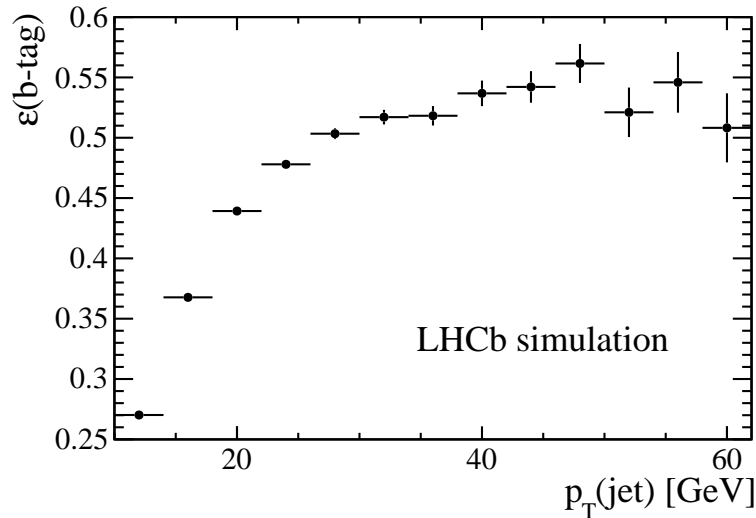


Figure 2: Efficiency of b-tagging as function of the jet transverse momentum. The uncertainties shown are statistical only.

transverse momentum and pseudorapidity. The value of $\varepsilon(\text{b-tag})$ shows little variation with pseudorapidity in the range $2.0 < \eta(\text{jet}) < 4.5$, while it rises strongly with p_T , reaching a value of 55% at high p_T , as shown in Fig. 2. The number of Z+b-jet events determined by the template fit is corrected for the b-tagging efficiency.

4 Systematic uncertainties

The systematic uncertainties related to the Z boson reconstruction, unfolding, jet energy calibration and final-state radiation are taken from Ref. [18]. Systematic uncertainties related to the M_{corr} templates modelling, b-tagging efficiency and jet efficiency flavour dependence are studied in this work.

The systematic uncertainty on the Z boson reconstruction takes account of the contributions from the track reconstruction, trigger efficiencies, muon identification efficiencies and the model used to fit the Z boson mass. The Z boson reconstruction systematic uncertainty is estimated to be 3.5% [18].

Migrations in the jet transverse momentum distribution are corrected for by unfolding. This correction is applied to the value of $\sigma(\text{Z+jet})$ measured in Ref. [18] and used in Eq. 1. Detailed studies show that no dedicated unfolding correction is necessary. The unfolding systematic uncertainty has two contributions. The difference between the SVD [23] and D’Agostini [24] unfolding methods is assigned as one contribution. The second contribution comes from the difference between the unfolded distribution and the true distribution in an independent simulated sample. This systematic uncertainty is taken from Ref. [18] and it is evaluated to be 1.5%.

An important contribution to the systematic uncertainties related to the jets comes

from the jet-energy scale. It is estimated by comparing the transverse momentum of the Z boson and the jet in single jet events, where their momenta are azimuthally opposed, and are expected to be balanced. An additional contribution of 2% to the jet-energy scale uncertainty comes from the differences between jets initiated from quarks and gluons. The systematic uncertainty of the jet identification is estimated by comparing the number of candidates in data and simulation with a more stringent selection. The total systematic uncertainty related to jets is 7.8% as estimated in Ref. [18].

The systematic uncertainty associated to final-state radiation is obtained by direct comparison to the simulation described above and an additional simulation, using HERWIG++ [25], as in Ref. [18]; it is estimated to be 0.2%. The systematic uncertainty associated with the knowledge of the luminosity is estimated to be 3.5% [26].

Possible systematic variations of the final result due to the extraction of $\varepsilon(\text{b-tag})$ and M_{corr} templates from simulations are controlled using two data samples enriched in b-jets and c-jets. The b-jet (c-jet) enriched sample is selected via one B^\pm (D^\pm) hadron candidate decaying to $J/\psi K^\pm$ ($K^\mp \pi^\pm \pi^\pm$) produced with a large azimuthal opening angle with respect to a probe jet. The b-tagging requirement is applied to the probe jet and a template fit is performed. Three studies are performed: 1) the data are divided into two ranges of M , the template fit is performed on each and the sum of the resulting b-jet yields is compared with the standard result; 2) a looser b-tagging requirement is applied and the b-jet yields after b-tagging efficiency correction are compared with the default values; and 3) the M_{corr} template is smeared to account for possible differences between simulation and data, and the impact on the b-jet yields is studied. The M_{corr} simulation modelling and TOPO candidate reconstruction efficiency studies are found to affect this measurement by up to 15%, where this uncertainty is dominated by the first of the studies mentioned above.

Using simulation, $\varepsilon(\text{Z+jet})/\varepsilon(\text{Z+b-jet})$ is found to be compatible with unity within 2%, which is taken as the systematic uncertainty due to the flavour dependence of the jet efficiency.

The systematic uncertainties are summarized in Table 1. They are added in quadrature leading to a total systematic error of 17.8%.

5 Results

We observe 179 (97) Z+jet events where at least one jet fulfils the b-tagging requirement for the $p_{\text{T}}(\text{jet}) > 10$ GeV (20 GeV) threshold. No events with more than one b-tagged jet are observed. The extended unbinned likelihood fit of the M_{corr} spectrum using Z+l-jet, Z+c-jet and Z+b-jet templates determines 72 ± 15 (39 ± 11) Z+b-jet events for the $p_{\text{T}}(\text{jet}) > 10$ GeV (20 GeV) threshold. The number of candidates corrected for b-tagging efficiency is found to be 177 ± 36 (76 ± 21) for the $p_{\text{T}}(\text{jet}) > 10$ GeV (20 GeV) threshold. Using the measurements of Ref. [18], we determine the cross-section of Z+b-jet production to be

$$\sigma(\text{Z}/\gamma^*(\mu^+\mu^-)+\text{b-jet}) = 295 \pm 60 \text{ (stat)} \pm 51 \text{ (syst)} \pm 10 \text{ (lumi) fb}$$

Table 1: Relative systematic uncertainty considered for the Z+b-jet cross-section for $p_{\text{T}}(\text{jet}) > 20 \text{ GeV}$. The relative uncertainties are similar for the 10 GeV threshold. The first four contributions are from Ref. [18].

Source of systematic uncertainty	Relative uncertainty (%)
Z boson reconstruction	3.5
Unfolding	1.5
Jet-energy scale, resolution and reconstruction	7.8
Final-state radiation	0.2
Luminosity	3.5
M_{corr} template and b-tagging	15.0
Jet reconstruction flavour dependence	2.0
Total	17.8

for $p_{\text{T}}(\text{jet}) > 10 \text{ GeV}$, and

$$\sigma(\text{Z}/\gamma^*(\mu^+\mu^-)+\text{b-jet}) = 128 \pm 36 \text{ (stat)} \pm 22 \text{ (syst)} \pm 5 \text{ (lumi) fb}$$

for $p_{\text{T}}(\text{jet}) > 20 \text{ GeV}$. These cross-sections are evaluated within the fiducial region $p_{\text{T}}(\mu) > 20 \text{ GeV}$, $60 \text{ GeV} < M(\mu^-\mu^+) < 120 \text{ GeV}$, $2.0 < \eta(\text{jet}) < 4.5$, $2.0 < \eta(\mu) < 4.5$ and $\Delta R(\text{jet}, \mu) > 0.4$.

The measurements are compared to predictions of the Z+b-jet cross-section calculated using MCFM [27] in the same kinematic range as for this measurement. The uncertainties include the PDF and theory uncertainties evaluated by varying independently the renormalization and factorization scales by a factor two around their nominal scales. Neither showering nor hadronization are included in MCFM; therefore the same kinematic requirements applied to jets in the data analysis are applied to the bottom quarks in MCFM. An overall correction is calculated by generating Z+b-jet events with PYTHIA v8.170 with the MSTW08 PDF set [28] where the same acceptance requirements are applied. Jets are reconstructed with FASTJET using the anti- k_{T} algorithm with $R = 0.5$ and then matched with a bottom quark, requiring $\Delta R(\text{jet}, \text{b-quark}) < 0.5$. The ratio between the number of events with at least one b-jet that fulfils the kinematic requirements of this measurement and the number of events with at least one b quark within the acceptance criteria are used as the fragmentation and hadronization correction for the MCFM predictions. The ratio is 0.77 (0.90) for $p_{\text{T}}(\text{jet}) > 10$ (20) GeV. Figure 3 shows the cross-section measurements compared to the LO calculation with massive bottom quarks and to LO and NLO calculations neglecting the bottom quark mass.

6 Summary

The cross-section for forward production of a Z boson or an off-shell photon, in the $\mu^+\mu^-$ channel, and a bottom-quark is measured in $\sqrt{s} = 7 \text{ TeV}$ proton-proton collisions

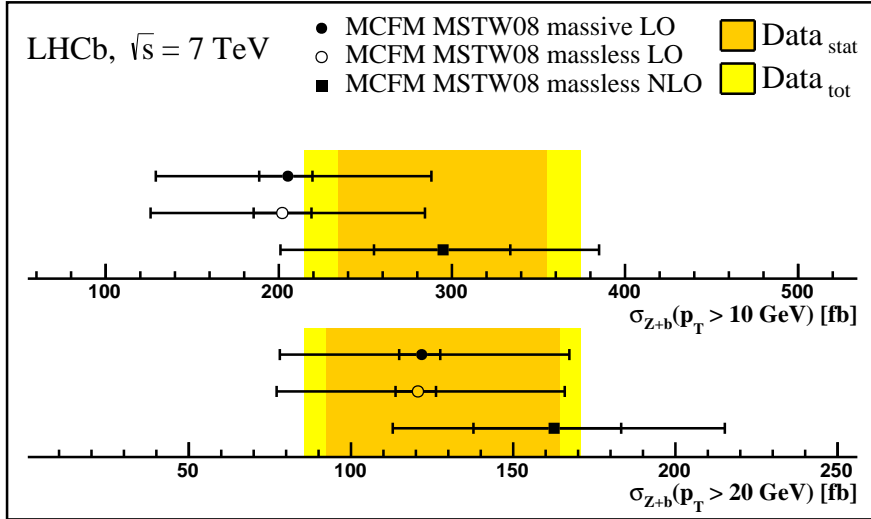


Figure 3: Z+b-jet cross-section for two $p_T(\text{jet})$ thresholds. The colour band shows the LHCb measurement (with the inner orange band showing the statistical uncertainty, and the outer yellow band showing the total uncertainty). The points with error bars correspond to the theoretical predictions with the inner error bars indicating their PDF uncertainties. These cross-sections are evaluated within the fiducial region $p_T(\mu) > 20$ GeV, $60 \text{ GeV} < M(\mu^-\mu^+) < 120$ GeV, $2 < \eta(\text{jet}) < 4.5$, $2 < \eta(\mu) < 4.5$ and $\Delta R(\text{jet}, \mu) > 0.4$.

corresponding to an integrated luminosity of 1.0 fb^{-1} of data collected in 2011 by the LHCb collaboration. Results are reported for the kinematic region $2.0 < \eta(\mu) < 4.5$, $p_T(\mu) > 20$ GeV, $60 < M(\mu^+\mu^-) < 120$ GeV, $p_T(\text{jet}) > 10(20)$ GeV, $2.0 < \eta(\text{jet}) < 4.5$ and $\Delta R(\text{jet}, \mu) > 0.4$. The measured cross-sections are

$$\sigma(Z/\gamma^*(\mu^+\mu^-)+\text{b-jet}) = 295 \pm 60 \text{ (stat)} \pm 51 \text{ (syst)} \pm 10 \text{ (lumi) fb}$$

for $p_T(\text{jet}) > 10$ GeV, and

$$\sigma(Z/\gamma^*(\mu^+\mu^-)+\text{b-jet}) = 128 \pm 36 \text{ (stat)} \pm 22 \text{ (syst)} \pm 5 \text{ (lumi) fb}$$

for $p_T(\text{jet}) > 20$ GeV.

The results are in agreement with MCFM predictions for massless and massive bottom quark calculations.

Acknowledgements

We express our gratitude to our colleagues in the CERN accelerator departments for the excellent performance of the LHC. We thank the technical and administrative staff at the LHCb institutes. We acknowledge support from CERN and from the national agencies: CAPES, CNPq, FAPERJ and FINEP (Brazil); NSFC (China); CNRS/IN2P3 (France);

BMBF, DFG, HGF and MPG (Germany); SFI (Ireland); INFN (Italy); FOM and NWO (The Netherlands); MNiSW and NCN (Poland); MEN/IFA (Romania); MinES and FANO (Russia); MinECo (Spain); SNSF and SER (Switzerland); NASU (Ukraine); STFC (United Kingdom); NSF (USA). The Tier1 computing centres are supported by IN2P3 (France), KIT and BMBF (Germany), INFN (Italy), NWO and SURF (The Netherlands), PIC (Spain), GridPP (United Kingdom). We are indebted to the communities behind the multiple open source software packages on which we depend. We are also thankful for the computing resources and the access to software R&D tools provided by Yandex LLC (Russia). Individual groups or members have received support from EPLANET, Marie Skłodowska-Curie Actions and ERC (European Union), Conseil général de Haute-Savoie, Labex ENIGMASS and OCEVU, Région Auvergne (France), RFBR (Russia), XuntaGal and GENCAT (Spain), Royal Society and Royal Commission for the Exhibition of 1851 (United Kingdom).

References

- [1] ATLAS collaboration, G. Aad *et al.*, *Measurement of the cross-section for b -jets produced in association with a Z boson at $\sqrt{s} = 7$ TeV with the ATLAS detector*, Phys. Lett. **B706** (2012) 295, [arXiv:1109.1403](#).
- [2] CMS collaboration, S. Chatrchyan *et al.*, *Measurement of the $Z/\gamma^* + b$ -jet cross section in pp collisions at 7 TeV*, JHEP **06** (2012) 126, [arXiv:1204.1643](#).
- [3] CDF collaboration, T. Aaltonen *et al.*, *Measurement of cross sections for b jet production in events with a Z boson in $p\bar{p}$ collisions at $\sqrt{s} = 1.96$ TeV*, Phys. Rev. **D79** (2009) 052008, [arXiv:0812.4458](#).
- [4] D0 collaboration, V. M. Abazov *et al.*, *Measurement of the ratio of differential cross sections $\sigma(pp \rightarrow Z + bjet)/\sigma(pp \rightarrow Z + jet)$ in $p\bar{p}$ collisions at $\sqrt{s} = 1.96$ TeV*, Phys. Rev. **D87** (2013) 092010, [arXiv:1301.2233](#).
- [5] LHCb collaboration, R. Aaij *et al.*, *First measurement of the charge asymmetry in beauty-quark pair production*, Phys. Rev. Lett. **113** (2014) 082003, [arXiv:1406.4789](#).
- [6] LHCb collaboration, A. A. Alves Jr. *et al.*, *The LHCb detector at the LHC*, JINST **3** (2008) S08005.
- [7] R. Aaij *et al.*, *Performance of the LHCb Vertex Locator*, JINST **9** (2014) P09007, [arXiv:1405.7808](#).
- [8] R. Arink *et al.*, *Performance of the LHCb Outer Tracker*, JINST **9** (2014) P01002, [arXiv:1311.3893](#).
- [9] M. Adinolfi *et al.*, *Performance of the LHCb RICH detector at the LHC*, Eur. Phys. J. **C73** (2013) 2431, [arXiv:1211.6759](#).

- [10] A. A. Alves Jr. *et al.*, *Performance of the LHCb muon system*, JINST **8** (2013) P02022, [arXiv:1211.1346](#).
- [11] R. Aaij *et al.*, *The LHCb trigger and its performance in 2011*, JINST **8** (2013) P04022, [arXiv:1211.3055](#).
- [12] T. Sjöstrand, S. Mrenna, and P. Skands, *PYTHIA 6.4 physics and manual*, JHEP **05** (2006) 026, [arXiv:hep-ph/0603175](#).
- [13] I. Belyaev *et al.*, *Handling of the generation of primary events in Gauss, the LHCb simulation framework*, Nuclear Science Symposium Conference Record (NSS/MIC) **IEEE** (2010) 1155.
- [14] P. M. Nadolsky *et al.*, *Implications of CTEQ global analysis for collider observables*, Phys. Rev. **D78** (2008) 013004, [arXiv:0802.0007](#).
- [15] D. J. Lange, *The EvtGen particle decay simulation package*, Nucl. Instrum. Meth. **A462** (2001) 152.
- [16] Geant4 collaboration, S. Agostinelli *et al.*, *Geant4: a simulation toolkit*, Nucl. Instrum. Meth. **A506** (2003) 250.
- [17] M. Clemencic *et al.*, *The LHCb simulation application, Gauss: Design, evolution and experience*, J. Phys. Conf. Ser. **331** (2011) 032023.
- [18] LHCb collaboration, R. Aaij *et al.*, *Study of forward Z +jet production in pp collisions at $\sqrt{s} = 7$ TeV*, JHEP **01** (2014) 033, [arXiv:1310.8197](#).
- [19] M. Cacciari, G. P. Salam, and G. Soyez, *The anti- k_t jet clustering algorithm*, JHEP **04** (2008) 063, [arXiv:0802.1189](#).
- [20] M. Cacciari, G. P. Salam, and G. Soyez, *FastJet user manual*, [arXiv:1111.6097](#).
- [21] V. V. Gligorov and M. Williams, *Efficient, reliable and fast high-level triggering using a bonsai boosted decision tree*, JINST **8** (2013) P02013, [arXiv:1210.6861](#).
- [22] M. Pivk and F. R. Le Diberder, *sPlot: a statistical tool to unfold data distributions*, Nucl. Instrum. Meth. **A555** (2005) 356, [arXiv:physics/0402083](#).
- [23] A. Hocker and V. Kartvelishvili, *SVD approach to data unfolding*, Nucl. Instrum. Meth. **A372** (1996) 469, [arXiv:hep-ph/9509307](#).
- [24] G. D'Agostini, *Unfolding of experimental distributions by an interactive use of Bayes's formula with intermediated smoothing*, Nucl. Instrum. Meth. **A362** (1995) 487.
- [25] M. Bahr *et al.*, *Herwig++ physics and manual*, Eur. Phys. J. **C58** (2008) 639, [arXiv:0803.0883](#).

- [26] LHCb collaboration, R. Aaij *et al.*, *Absolute luminosity measurements with the LHCb detector at the LHC*, JINST **7** (2012) P01010, [arXiv:1110.2866](#).
- [27] J. M. Campbell and R. Ellis, *MCFM for the Tevatron and the LHC*, Nucl. Phys. Proc. **557** (2010) 205, [arXiv:1007.3492](#).
- [28] A. D. Martin, W. J. Stirling, R. S. Thorne, and G. Watt, *Parton distributions for the LHC*, Eur. Phys. J. **C63** (2009) 189, [arXiv:0901.0002](#).

LHCb collaboration

R. Aaij⁴¹, B. Adeva³⁷, M. Adinolfi⁴⁶, A. Affolder⁵², Z. Ajaltouni⁵, S. Akar⁶, J. Albrecht⁹, F. Alessio³⁸, M. Alexander⁵¹, S. Ali⁴¹, G. Alkhazov³⁰, P. Alvarez Cartelle³⁷, A.A. Alves Jr^{25,38}, S. Amato², S. Amerio²², Y. Amhis⁷, L. An³, L. Anderlini^{17,g}, J. Anderson⁴⁰, R. Andreassen⁵⁷, M. Andreotti^{16,f}, J.E. Andrews⁵⁸, R.B. Appleby⁵⁴, O. Aquines Gutierrez¹⁰, F. Archilli³⁸, A. Artamonov³⁵, M. Artuso⁵⁹, E. Aslanides⁶, G. Auriemma^{25,n}, M. Baalouch⁵, S. Bachmann¹¹, J.J. Back⁴⁸, A. Badalov³⁶, C. Baesso⁶⁰, W. Baldini¹⁶, R.J. Barlow⁵⁴, C. Barschel³⁸, S. Barsuk⁷, W. Barter⁴⁷, V. Batozskaya²⁸, V. Battista³⁹, A. Bay³⁹, L. Beaucourt⁴, J. Beddow⁵¹, F. Bedeschi²³, I. Bediaga¹, S. Belogurov³¹, K. Belous³⁵, I. Belyaev³¹, E. Ben-Haim⁸, G. Bencivenni¹⁸, S. Benson³⁸, J. Benton⁴⁶, A. Berezhnoy³², R. Bernet⁴⁰, AB Bertolin²², M.-O. Bettler⁴⁷, M. van Beuzekom⁴¹, A. Bien¹¹, S. Bifani⁴⁵, T. Bird⁵⁴, A. Bizzeti^{17,i}, P.M. Bjørnstad⁵⁴, T. Blake⁴⁸, F. Blanc³⁹, J. Blouw¹⁰, S. Blusk⁵⁹, V. Bocci²⁵, A. Bondar³⁴, N. Bondar^{30,38}, W. Bonivento¹⁵, S. Borghi⁵⁴, A. Borgia⁵⁹, M. Borsato⁷, T.J.V. Bowcock⁵², E. Bowen⁴⁰, C. Bozzi¹⁶, D. Brett⁵⁴, M. Britsch¹⁰, T. Britton⁵⁹, J. Brodzicka⁵⁴, N.H. Brook⁴⁶, A. Bursche⁴⁰, J. Buytaert³⁸, S. Cadeddu¹⁵, R. Calabrese^{16,f}, M. Calvi^{20,k}, M. Calvo Gomez^{36,p}, P. Campana¹⁸, D. Campora Perez³⁸, L. Capriotti⁵⁴, A. Carbone^{14,d}, G. Carboni^{24,l}, R. Cardinale^{19,38,j}, A. Cardini¹⁵, L. Carson⁵⁰, K. Carvalho Akiba^{2,38}, RCM Casanova Mohr³⁶, G. Casse⁵², L. Cassina^{20,k}, L. Castillo Garcia³⁸, M. Cattaneo³⁸, Ch. Cauet⁹, R. Cenci^{23,t}, M. Charles⁸, Ph. Charpentier³⁸, M. Chefdeville⁴, S. Chen⁵⁴, S.-F. Cheung⁵⁵, N. Chiapolini⁴⁰, M. Chrzaszcz^{40,26}, X. Cid Vidal³⁸, G. Ciezarek⁴¹, P.E.L. Clarke⁵⁰, M. Clemencic³⁸, H.V. Cliff⁴⁷, J. Closier³⁸, V. Coco³⁸, J. Cogan⁶, E. Cogneras⁵, V. Cogoni¹⁵, L. Cojocariu²⁹, G. Collazuol²², P. Collins³⁸, A. Comerma-Montells¹¹, A. Contu^{15,38}, A. Cook⁴⁶, M. Coombes⁴⁶, S. Coquereau⁸, G. Corti³⁸, M. Corvo^{16,f}, I. Counts⁵⁶, B. Couturier³⁸, G.A. Cowan⁵⁰, D.C. Craik⁴⁸, A.C. Crocombe⁴⁸, M. Cruz Torres⁶⁰, S. Cunliffe⁵³, R. Currie⁵³, C. D'Ambrosio³⁸, J. Dalseno⁴⁶, P. David⁸, P.N.Y. David⁴¹, A. Davis⁵⁷, K. De Bruyn⁴¹, S. De Capua⁵⁴, M. De Cian¹¹, J.M. De Miranda¹, L. De Paula², W. De Silva⁵⁷, P. De Simone¹⁸, C.-T. Dean⁵¹, D. Decamp⁴, M. Deckenhoff⁹, L. Del Buono⁸, N. Déléage⁴, D. Derkach⁵⁵, O. Deschamps⁵, F. Dettori³⁸, B. Dey⁴⁰, A. Di Canto³⁸, A Di Domenico²⁵, H. Dijkstra³⁸, S. Donleavy⁵², F. Dordei¹¹, M. Dorigo³⁹, A. Dosil Suárez³⁷, D. Dossett⁴⁸, A. Dovbnya⁴³, K. Dreimanis⁵², G. Dujany⁵⁴, F. Dupertuis³⁹, P. Durante³⁸, R. Dzhelyadin³⁵, A. Dziurda²⁶, A. Dzyuba³⁰, S. Easo^{49,38}, U. Egede⁵³, V. Egorychev³¹, S. Eidelman³⁴, S. Eisenhardt⁵⁰, U. Eitschberger⁹, R. Ekelhof⁹, L. Eklund⁵¹, I. El Rifai⁵, Ch. Elsasser⁴⁰, S. Ely⁵⁹, S. Esen¹¹, H.-M. Evans⁴⁷, T. Evans⁵⁵, A. Falabella¹⁴, C. Färber¹¹, C. Farinelli⁴¹, N. Farley⁴⁵, S. Farry⁵², R. Fay⁵², D. Ferguson⁵⁰, V. Fernandez Albor³⁷, F. Ferreira Rodrigues¹, M. Ferro-Luzzi³⁸, S. Filippov³³, M. Fiore^{16,f}, M. Fiorini^{16,f}, M. Firlej²⁷, C. Fitzpatrick³⁹, T. Fiutowski²⁷, P. Fol⁵³, M. Fontana¹⁰, F. Fontanelli^{19,j}, R. Forty³⁸, O. Francisco², M. Frank³⁸, C. Frei³⁸, M. Frosini^{17,g}, J. Fu^{21,38}, E. Furfaro^{24,l}, A. Gallas Torreira³⁷, D. Galli^{14,d}, S. Gallorini^{22,38}, S. Gambetta^{19,j}, M. Gandelman², P. Gandini⁵⁹, Y. Gao³, J. García Pardiñas³⁷, J. Garofoli⁵⁹, J. Garra Tico⁴⁷, L. Garrido³⁶, D. Gascon³⁶, C. Gaspar³⁸, U. Gastaldi¹⁶, R. Gauld⁵⁵, L. Gavardi⁹, G. Gazzoni⁵, A. Geraci^{21,v}, E. Gersabeck¹¹, M. Gersabeck⁵⁴, T. Gershon⁴⁸, Ph. Ghez⁴, A. Gianelle²², S. Giani³⁹, V. Gibson⁴⁷, L. Giubega²⁹, V.V. Gligorov³⁸, C. Göbel⁶⁰, D. Golubkov³¹, A. Golutvin^{53,31,38}, A. Gomes^{1,a}, C. Gotti^{20,k}, M. Grabalosa Gándara⁵, R. Graciani Diaz³⁶, L.A. Granado Cardoso³⁸, E. Graugés³⁶, E. Graverini⁴⁰, G. Graziani¹⁷, A. Grecu²⁹, E. Greening⁵⁵, S. Gregson⁴⁷, P. Griffith⁴⁵, L. Grillo¹¹, O. Grünberg⁶³, B. Gui⁵⁹, E. Gushchin³³, Yu. Guz^{35,38}, T. Gys³⁸, C. Hadjivasiliou⁵⁹, G. Haefeli³⁹, C. Haen³⁸, S.C. Haines⁴⁷, S. Hall⁵³, B. Hamilton⁵⁸,

T. Hampson⁴⁶, X. Han¹¹, S. Hansmann-Menzemer¹¹, N. Harnew⁵⁵, S.T. Harnew⁴⁶, J. Harrison⁵⁴,
 J. He³⁸, T. Head³⁹, V. Heijne⁴¹, K. Hennessy⁵², P. Henrard⁵, L. Henry⁸,
 J.A. Hernando Morata³⁷, E. van Herwijnen³⁸, M. Heß⁶³, A. Hicheur², D. Hill⁵⁵, M. Hoballah⁵,
 C. Hombach⁵⁴, W. Hulsbergen⁴¹, N. Hussain⁵⁵, D. Hutchcroft⁵², D. Hynds⁵¹, M. Idzik²⁷,
 P. Ilten⁵⁶, R. Jacobsson³⁸, A. Jaeger¹¹, J. Jalocha⁵⁵, E. Jans⁴¹, A. Jawahery⁵⁸, F. Jing³,
 M. John⁵⁵, D. Johnson³⁸, C.R. Jones⁴⁷, C. Joram³⁸, B. Jost³⁸, N. Jurik⁵⁹, S. Kandybei⁴³,
 W. Kanso⁶, M. Karacson³⁸, T.M. Karbach³⁸, S. Karodia⁵¹, M. Kelsey⁵⁹, I.R. Kenyon⁴⁵,
 T. Ketel⁴², B. Khanji^{20,38,k}, C. Khurewathanakul³⁹, S. Klaver⁵⁴, K. Klimaszewski²⁸,
 O. Kochebina⁷, M. Kolpin¹¹, I. Komarov³⁹, R.F. Koopman⁴², P. Koppenburg^{41,38}, M. Korolev³²,
 L. Kravchuk³³, K. Kreplin¹¹, M. Kreps⁴⁸, G. Krocker¹¹, P. Krokovny³⁴, F. Kruse⁹,
 W. Kucewicz^{26,o}, M. Kucharczyk^{20,26,k}, V. Kudryavtsev³⁴, K. Kurek²⁸, T. Kvaratskheliya³¹,
 V.N. La Thi³⁹, D. Lacarrere³⁸, G. Lafferty⁵⁴, A. Lai¹⁵, D. Lambert⁵⁰, R.W. Lambert⁴²,
 G. Lanfranchi¹⁸, C. Langenbruch⁴⁸, B. Langhans³⁸, T. Latham⁴⁸, C. Lazzeroni⁴⁵, R. Le Gac⁶,
 J. van Leerdam⁴¹, J.-P. Lees⁴, R. Lefèvre⁵, A. Leflat³², J. Lefrançois⁷, O. Leroy⁶, T. Lesiak²⁶,
 B. Leverington¹¹, Y. Li⁷, T. Likhomanenko⁶⁴, M. Liles⁵², R. Lindner³⁸, C. Linn³⁸, F. Lionetto⁴⁰,
 B. Liu¹⁵, S. Lohn³⁸, I. Longstaff⁵¹, J.H. Lopes², P. Lowdon⁴⁰, D. Lucchesi^{22,r}, H. Luo⁵⁰,
 A. Lupato²², E. Luppi^{16,f}, O. Lupton⁵⁵, F. Machefert⁷, I.V. Machikhiliyan³¹, F. Maciuc²⁹,
 O. Maev³⁰, S. Malde⁵⁵, A. Malinin⁶⁴, G. Manca^{15,e}, G. Mancinelli⁶, A. Mapelli³⁸, J. Maratas⁵,
 J.F. Marchand⁴, U. Marconi¹⁴, C. Marin Benito³⁶, P. Marino^{23,t}, R. Märki³⁹, J. Marks¹¹,
 G. Martellotti²⁵, M. Martinelli³⁹, D. Martinez Santos⁴², F. Martinez Vidal⁶⁵,
 D. Martins Tostes², A. Massafferri¹, R. Matev³⁸, Z. Mathe³⁸, C. Matteuzzi²⁰, A. Mazurov⁴⁵,
 M. McCann⁵³, J. McCarthy⁴⁵, A. McNab⁵⁴, R. McNulty¹², B. McSkelly⁵², B. Meadows⁵⁷,
 F. Meier⁹, M. Meissner¹¹, M. Merk⁴¹, D.A. Milanes⁶², M.-N. Minard⁴, N. Moggi¹⁴,
 J. Molina Rodriguez⁶⁰, S. Monteil⁵, M. Morandin²², P. Morawski²⁷, A. Mordà⁶, M.J. Morello^{23,t},
 J. Moron²⁷, A.-B. Morris⁵⁰, R. Mountain⁵⁹, F. Muheim⁵⁰, K. Müller⁴⁰, M. Mussini¹⁴,
 B. Muster³⁹, P. Naik⁴⁶, T. Nakada³⁹, R. Nandakumar⁴⁹, I. Nasteva², M. Needham⁵⁰, N. Neri²¹,
 S. Neubert³⁸, N. Neufeld³⁸, M. Neuner¹¹, A.D. Nguyen³⁹, T.D. Nguyen³⁹, C. Nguyen-Mau^{39,q},
 M. Nicol⁷, V. Niess⁵, R. Niet⁹, N. Nikitin³², T. Nikodem¹¹, A. Novoselov³⁵, D.P. O’Hanlon⁴⁸,
 A. Oblakowska-Mucha²⁷, V. Obraztsov³⁵, S. Ogilvy⁵¹, O. Okhrimenko⁴⁴, R. Oldeman^{15,e},
 C.J.G. Onderwater⁶⁶, M. Orlandea²⁹, B. Osorio Rodrigues¹, J.M. Otalora Goicochea²,
 A. Otto³⁸, P. Owen⁵³, A. Oyanguren⁶⁵, B.K. Pal⁵⁹, A. Palano^{13,c}, F. Palombo^{21,u}, M. Palutan¹⁸,
 J. Panman³⁸, A. Papanestis^{49,38}, M. Pappagallo⁵¹, L.L. Pappalardo^{16,f}, C. Parkes⁵⁴,
 C.J. Parkinson^{9,45}, G. Passaleva¹⁷, G.D. Patel⁵², M. Patel⁵³, C. Patrignani^{19,j}, A. Pearce⁵⁴,
 A. Pellegrino⁴¹, G. Penso^{25,m}, M. Pepe Altarelli³⁸, S. Perazzini^{14,d}, P. Perret⁵, L. Pescatore⁴⁵,
 E. Pesen⁶⁷, K. Petridis⁵³, A. Petrolini^{19,j}, E. Picatoste Olloqui³⁶, B. Pietrzyk⁴, T. Pilař⁴⁸,
 D. Pinci²⁵, A. Pistone¹⁹, S. Playfer⁵⁰, M. Plo Casasus³⁷, F. Polci⁸, A. Poluektov^{48,34},
 I. Polyakov³¹, E. Polycarpo², A. Popov³⁵, D. Popov¹⁰, B. Popovici²⁹, C. Potterat², E. Price⁴⁶,
 J.D. Price⁵², J. Prisciandaro³⁹, A. Pritchard⁵², C. Prouve⁴⁶, V. Pugatch⁴⁴, A. Puig Navarro³⁹,
 G. Punzi^{23,s}, W. Qian⁴, B. Rachwal²⁶, J.H. Rademacker⁴⁶, B. Rakotomiamanana³⁹,
 M. Rama²³, M.S. Rangel², I. Raniuk⁴³, N. Rauschmayr³⁸, G. Raven⁴², F. Redi⁵³, S. Reichert⁵⁴,
 M.M. Reid⁴⁸, A.C. dos Reis¹, S. Ricciardi⁴⁹, S. Richards⁴⁶, M. Rihl³⁸, K. Rinnert⁵²,
 V. Rives Molina³⁶, P. Robbe⁷, A.B. Rodrigues¹, E. Rodrigues⁵⁴, P. Rodriguez Perez⁵⁴,
 S. Roiser³⁸, V. Romanovsky³⁵, A. Romero Vidal³⁷, M. Rotondo²², J. Rouvinet³⁹, T. Ruf³⁸,
 H. Ruiz³⁶, P. Ruiz Valls⁶⁵, J.J. Saborido Silva³⁷, N. Sagidova³⁰, P. Sail⁵¹, B. Saitta^{15,e},
 V. Salustino Guimaraes², C. Sanchez Mayordomo⁶⁵, B. Sanmartin Sedes³⁷, R. Santacesaria²⁵,
 C. Santamarina Rios³⁷, E. Santovetti^{24,l}, A. Sarti^{18,m}, C. Satriano^{25,n}, A. Satta²⁴,

D.M. Saunders⁴⁶, D. Savrina^{31,32}, M. Schiller³⁸, H. Schindler³⁸, M. Schlupp⁹, M. Schmelling¹⁰, B. Schmidt³⁸, O. Schneider³⁹, A. Schopper³⁸, M.-H. Schune⁷, R. Schwemmer³⁸, B. Sciascia¹⁸, A. Sciubba^{25,m}, A. Semennikov³¹, I. Sepp⁵³, N. Serra⁴⁰, J. Serrano⁶, L. Sestini²², P. Seyfert¹¹, M. Shapkin³⁵, I. Shapoval^{16,43,f}, Y. Shcheglov³⁰, T. Shears⁵², L. Shekhtman³⁴, V. Shevchenko⁶⁴, A. Shires⁹, R. Silva Coutinho⁴⁸, G. Simi²², M. Sirendi⁴⁷, N. Skidmore⁴⁶, I. Skillicorn⁵¹, T. Skwarnicki⁵⁹, N.A. Smith⁵², E. Smith^{55,49}, E. Smith⁵³, J. Smith⁴⁷, M. Smith⁵⁴, H. Snoek⁴¹, M.D. Sokoloff⁵⁷, F.J.P. Soler⁵¹, F. Soomro³⁹, D. Souza⁴⁶, B. Souza De Paula², B. Spaan⁹, P. Spradlin⁵¹, S. Sridharan³⁸, F. Stagni³⁸, M. Stahl¹¹, S. Stahl¹¹, O. Steinkamp⁴⁰, O. Stenyakin³⁵, F. Sterpka⁵⁹, S. Stevenson⁵⁵, S. Stoica²⁹, S. Stone⁵⁹, B. Storaci⁴⁰, S. Stracka^{23,t}, M. Straticiu²⁹, U. Straumann⁴⁰, R. Stroili²², L. Sun⁵⁷, W. Sutcliffe⁵³, K. Swientek²⁷, S. Swientek⁹, V. Syropoulos⁴², M. Szczekowski²⁸, P. Szczypka^{39,38}, T. Szumlak²⁷, S. T’Jampens⁴, M. Teklishyn⁷, G. Tellarini^{16,f}, F. Teubert³⁸, C. Thomas⁵⁵, E. Thomas³⁸, J. van Tilburg⁴¹, V. Tisserand⁴, M. Tobin³⁹, J. Todd⁵⁷, S. Tolk⁴², L. Tomassetti^{16,f}, D. Tonelli³⁸, S. Topp-Joergensen⁵⁵, N. Torr⁵⁵, E. Tournefier⁴, S. Tourneur³⁹, M.T. Tran³⁹, M. Tresch⁴⁰, A. Trisovic³⁸, A. Tsaregorodtsev⁶, P. Tsopelas⁴¹, N. Tuning⁴¹, M. Ubeda Garcia³⁸, A. Ukleja²⁸, A. Ustyuzhanin⁶⁴, U. Uwer¹¹, C. Vacca¹⁵, V. Vagnoni¹⁴, G. Valenti¹⁴, A. Vallier⁷, R. Vazquez Gomez¹⁸, P. Vazquez Regueiro³⁷, C. Vázquez Sierra³⁷, S. Vecchi¹⁶, J.J. Velthuis⁴⁶, M. Veltri^{17,h}, G. Veneziano³⁹, M. Vesterinen¹¹, JVV B Viana Barbosa³⁸, B. Viaud⁷, D. Vieira², M. Vieites Diaz³⁷, X. Vilasis-Cardona^{36,p}, A. Vollhardt⁴⁰, D. Volyanskyy¹⁰, D. Voong⁴⁶, A. Vorobyev³⁰, V. Vorobyev³⁴, C. Voß⁶³, J.A. de Vries⁴¹, R. Waldi⁶³, C. Wallace⁴⁸, R. Wallace¹², J. Walsh²³, S. Wandernoth¹¹, J. Wang⁵⁹, D.R. Ward⁴⁷, N.K. Watson⁴⁵, D. Websdale⁵³, M. Whitehead⁴⁸, D. Wiedner¹¹, G. Wilkinson^{55,38}, M. Wilkinson⁵⁹, M.P. Williams⁴⁵, M. Williams⁵⁶, H.W. Wilschut⁶⁶, F.F. Wilson⁴⁹, J. Wimberley⁵⁸, J. Wishahi⁹, W. Wislicki²⁸, M. Witek²⁶, G. Wormser⁷, S.A. Wotton⁴⁷, S. Wright⁴⁷, K. Wyllie³⁸, Y. Xie⁶¹, Z. Xing⁵⁹, Z. Xu³⁹, Z. Yang³, X. Yuan³, O. Yushchenko³⁵, M. Zangoli¹⁴, M. Zavertyaev^{10,b}, L. Zhang³, W.C. Zhang¹², Y. Zhang³, A. Zhelezov¹¹, A. Zhokhov³¹, L. Zhong³.

¹ Centro Brasileiro de Pesquisas Físicas (CBPF), Rio de Janeiro, Brazil

² Universidade Federal do Rio de Janeiro (UFRJ), Rio de Janeiro, Brazil

³ Center for High Energy Physics, Tsinghua University, Beijing, China

⁴ LAPP, Université de Savoie, CNRS/IN2P3, Annecy-Le-Vieux, France

⁵ Clermont Université, Université Blaise Pascal, CNRS/IN2P3, LPC, Clermont-Ferrand, France

⁶ CPPM, Aix-Marseille Université, CNRS/IN2P3, Marseille, France

⁷ LAL, Université Paris-Sud, CNRS/IN2P3, Orsay, France

⁸ LPNHE, Université Pierre et Marie Curie, Université Paris Diderot, CNRS/IN2P3, Paris, France

⁹ Fakultät Physik, Technische Universität Dortmund, Dortmund, Germany

¹⁰ Max-Planck-Institut für Kernphysik (MPIK), Heidelberg, Germany

¹¹ Physikalisches Institut, Ruprecht-Karls-Universität Heidelberg, Heidelberg, Germany

¹² School of Physics, University College Dublin, Dublin, Ireland

¹³ Sezione INFN di Bari, Bari, Italy

¹⁴ Sezione INFN di Bologna, Bologna, Italy

¹⁵ Sezione INFN di Cagliari, Cagliari, Italy

¹⁶ Sezione INFN di Ferrara, Ferrara, Italy

¹⁷ Sezione INFN di Firenze, Firenze, Italy

¹⁸ Laboratori Nazionali dell’INFN di Frascati, Frascati, Italy

¹⁹ Sezione INFN di Genova, Genova, Italy

²⁰ Sezione INFN di Milano Bicocca, Milano, Italy

²¹ Sezione INFN di Milano, Milano, Italy

²² Sezione INFN di Padova, Padova, Italy

- ²³ *Sezione INFN di Pisa, Pisa, Italy*
- ²⁴ *Sezione INFN di Roma Tor Vergata, Roma, Italy*
- ²⁵ *Sezione INFN di Roma La Sapienza, Roma, Italy*
- ²⁶ *Henryk Niewodniczanski Institute of Nuclear Physics Polish Academy of Sciences, Kraków, Poland*
- ²⁷ *AGH - University of Science and Technology, Faculty of Physics and Applied Computer Science, Kraków, Poland*
- ²⁸ *National Center for Nuclear Research (NCBJ), Warsaw, Poland*
- ²⁹ *Horia Hulubei National Institute of Physics and Nuclear Engineering, Bucharest-Magurele, Romania*
- ³⁰ *Petersburg Nuclear Physics Institute (PNPI), Gatchina, Russia*
- ³¹ *Institute of Theoretical and Experimental Physics (ITEP), Moscow, Russia*
- ³² *Institute of Nuclear Physics, Moscow State University (SINP MSU), Moscow, Russia*
- ³³ *Institute for Nuclear Research of the Russian Academy of Sciences (INR RAN), Moscow, Russia*
- ³⁴ *Budker Institute of Nuclear Physics (SB RAS) and Novosibirsk State University, Novosibirsk, Russia*
- ³⁵ *Institute for High Energy Physics (IHEP), Protvino, Russia*
- ³⁶ *Universitat de Barcelona, Barcelona, Spain*
- ³⁷ *Universidad de Santiago de Compostela, Santiago de Compostela, Spain*
- ³⁸ *European Organization for Nuclear Research (CERN), Geneva, Switzerland*
- ³⁹ *Ecole Polytechnique Fédérale de Lausanne (EPFL), Lausanne, Switzerland*
- ⁴⁰ *Physik-Institut, Universität Zürich, Zürich, Switzerland*
- ⁴¹ *Nikhef National Institute for Subatomic Physics, Amsterdam, The Netherlands*
- ⁴² *Nikhef National Institute for Subatomic Physics and VU University Amsterdam, Amsterdam, The Netherlands*
- ⁴³ *NSC Kharkiv Institute of Physics and Technology (NSC KIPT), Kharkiv, Ukraine*
- ⁴⁴ *Institute for Nuclear Research of the National Academy of Sciences (KINR), Kyiv, Ukraine*
- ⁴⁵ *University of Birmingham, Birmingham, United Kingdom*
- ⁴⁶ *H.H. Wills Physics Laboratory, University of Bristol, Bristol, United Kingdom*
- ⁴⁷ *Cavendish Laboratory, University of Cambridge, Cambridge, United Kingdom*
- ⁴⁸ *Department of Physics, University of Warwick, Coventry, United Kingdom*
- ⁴⁹ *STFC Rutherford Appleton Laboratory, Didcot, United Kingdom*
- ⁵⁰ *School of Physics and Astronomy, University of Edinburgh, Edinburgh, United Kingdom*
- ⁵¹ *School of Physics and Astronomy, University of Glasgow, Glasgow, United Kingdom*
- ⁵² *Oliver Lodge Laboratory, University of Liverpool, Liverpool, United Kingdom*
- ⁵³ *Imperial College London, London, United Kingdom*
- ⁵⁴ *School of Physics and Astronomy, University of Manchester, Manchester, United Kingdom*
- ⁵⁵ *Department of Physics, University of Oxford, Oxford, United Kingdom*
- ⁵⁶ *Massachusetts Institute of Technology, Cambridge, MA, United States*
- ⁵⁷ *University of Cincinnati, Cincinnati, OH, United States*
- ⁵⁸ *University of Maryland, College Park, MD, United States*
- ⁵⁹ *Syracuse University, Syracuse, NY, United States*
- ⁶⁰ *Pontifícia Universidade Católica do Rio de Janeiro (PUC-Rio), Rio de Janeiro, Brazil, associated to ²*
- ⁶¹ *Institute of Particle Physics, Central China Normal University, Wuhan, Hubei, China, associated to ³*
- ⁶² *Departamento de Física, Universidad Nacional de Colombia, Bogota, Colombia, associated to ⁸*
- ⁶³ *Institut für Physik, Universität Rostock, Rostock, Germany, associated to ¹¹*
- ⁶⁴ *National Research Centre Kurchatov Institute, Moscow, Russia, associated to ³¹*
- ⁶⁵ *Instituto de Física Corpuscular (IFIC), Universitat de Valencia-CSIC, Valencia, Spain, associated to ³⁶*
- ⁶⁶ *Van Swinderen Institute, University of Groningen, Groningen, The Netherlands, associated to ⁴¹*
- ⁶⁷ *Celal Bayar University, Manisa, Turkey, associated to ³⁸*

^a *Universidade Federal do Triângulo Mineiro (UFTM), Uberaba-MG, Brazil*

^b *P.N. Lebedev Physical Institute, Russian Academy of Science (LPI RAS), Moscow, Russia*

^c *Università di Bari, Bari, Italy*

^d *Università di Bologna, Bologna, Italy*

- ^e *Università di Cagliari, Cagliari, Italy*
- ^f *Università di Ferrara, Ferrara, Italy*
- ^g *Università di Firenze, Firenze, Italy*
- ^h *Università di Urbino, Urbino, Italy*
- ⁱ *Università di Modena e Reggio Emilia, Modena, Italy*
- ^j *Università di Genova, Genova, Italy*
- ^k *Università di Milano Bicocca, Milano, Italy*
- ^l *Università di Roma Tor Vergata, Roma, Italy*
- ^m *Università di Roma La Sapienza, Roma, Italy*
- ⁿ *Università della Basilicata, Potenza, Italy*
- ^o *AGH - University of Science and Technology, Faculty of Computer Science, Electronics and Telecommunications, Kraków, Poland*
- ^p *LIFAELS, La Salle, Universitat Ramon Llull, Barcelona, Spain*
- ^q *Hanoi University of Science, Hanoi, Viet Nam*
- ^r *Università di Padova, Padova, Italy*
- ^s *Università di Pisa, Pisa, Italy*
- ^t *Scuola Normale Superiore, Pisa, Italy*
- ^u *Università degli Studi di Milano, Milano, Italy*
- ^v *Politecnico di Milano, Milano, Italy*